Bulletin of the Natural History Museum, 2021, 14: 45-61.
Received 1 Nov 2021; Accepted 11 Nov 2021.

doi:10.5937/bnhmb2114045A
UDC: 902.2:550.837(497.11)
903.4"634"(497.11)

Original scientific paper

2D ELECTRICAL IMAGING INVESTIGATIONS AT THE NEOLITHIC SETTLEMENT "PLOČNIK"

FILIP ARNAUT, BRANISLAV SRETENOVIĆ

University of Belgrade, Faculty of Mining and Geology, Department of Geophysics, Đušina 7, Belgrade, Serbia
G601-20@rgf.bg.ac.rs, branislav.sretenovic@rgf.bg.ac.rs

At the Neolithic settlement "Pločnik" near Prokuplje in Serbia, the electrical imaging method (ERT) was deployed. At the sounding site S-3, 1D electrical survey revealed a low resistivity layer with a thickness of 0.8 meters and a resistivity of about 30 Ωm. A sharp and steep boundary divides the high resistivity medium and the low resistivity medium, according to the 2D electrical survey. The resolution of the ERT method was tested using 3D forward and inverse modeling to see whether it could distinguish the high resistivity pit from the surrounding high resistivity gravel.

Key words: Electrical imaging (ERT), Neolithic settlement "Pločnik", Forward modelling, Inverse modelling.

INTRODUCTION

The archaeological Neolithic settlement "Pločnik" is located near the town of Prokuplje in central Serbia, covering an area of about 80 hectares

and belonging to the well-known "Vinča" culture. Earlier archeological investigations, which were carried out in the traditional way by digging archeological trenches at several sites, revealed the presence of a large settlement and, more importantly, the possibility of metallurgy operations. The discovery of various copper tools and jewelry, as well as copper ores and minerals (chalcopyrite, malachite), is linked to the open-profile conical and cylindrical pits with diameters up to 9 meters and depths of 3.5-4 meters at the vertical cliff. These pits have been filled with ash deposits, most likely as a result of copper processing. Smaller and shallower pits (with diameters up to 3 meters and depths of 1.5-3 meters) are also present, often containing animal bones, pottery fragments, and anthropomorphic terracotta (Vukadinovich *et al.*, 1999).

Given the size of the potential targets, their burial depths, and the potential contrast of their physical properties with the surrounding material, it was agreed to use electrical mapping to detect relatively large pits filled with ash. The geophysical methods used successfully identified the most important anomalous zones and significantly reduced the region available for possible archeological, 2D, and 3D geoelectrical scanning investigations.

LOCATION AND GEOLOGICAL SETTING OF THE SURVEY AREA

Figure 1a depicts the survey area, which includes two sublocalities (Pločnik I and Pločnik II) where the survey was conducted. The findings from the Pločnik I locality will be presented in this research paper. Figure 1b shows an archeological profile discovered as a result of coastal erosion along the river Toplica. The existence of a pit with a radius of a few meters and a depth of about 4 meters can be clearly seen.

The vertical cliff formed by the river flow reveals a basic geological structure consisting of an almost homogeneous loess-like, four- to five-meter-thick clayey layer that covers the alluvial gravel of the Toplica river. This fact greatly improves the possibility of successful application of the geophysical methods by reducing the geological interference in delineating anomalies caused by archeological remainders.

1D GEOELECTRICAL SURVEY RESULTS

The inquiry was approached in a variety of ways at the survey location (Figure 2). Geoelectrical mapping, as well as 2D electrical imaging and vertical electrical sounding (VES) were deployed. There were twelve parallel geoelectrical mapping profiles (I-XII), four electrical imaging

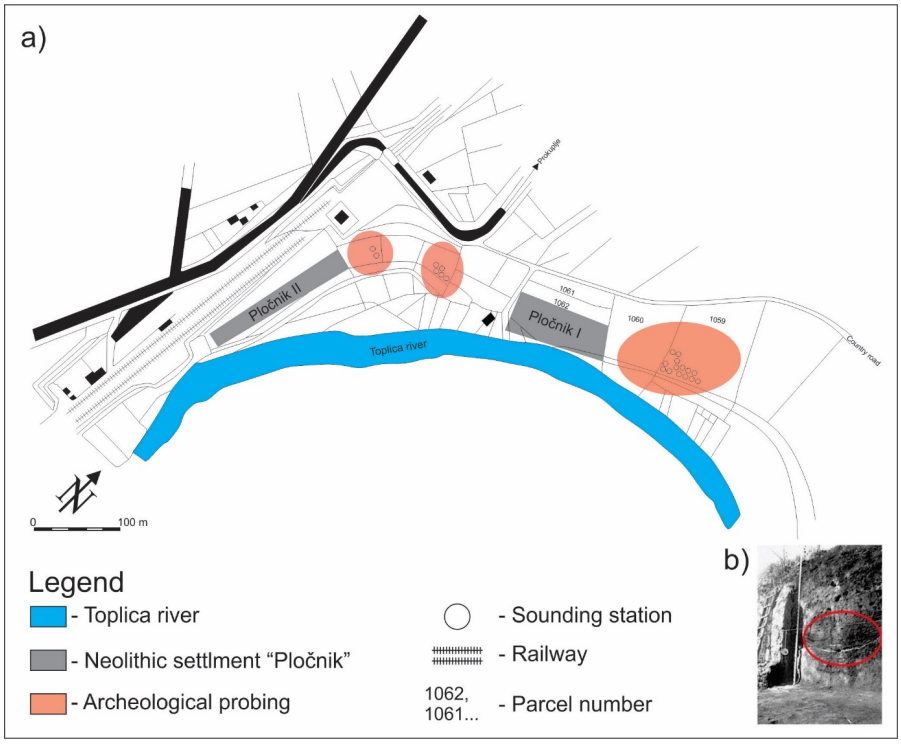

Fig. 1. – (a) The location of the survey area; (b) the archeological profile with the marked pit location.

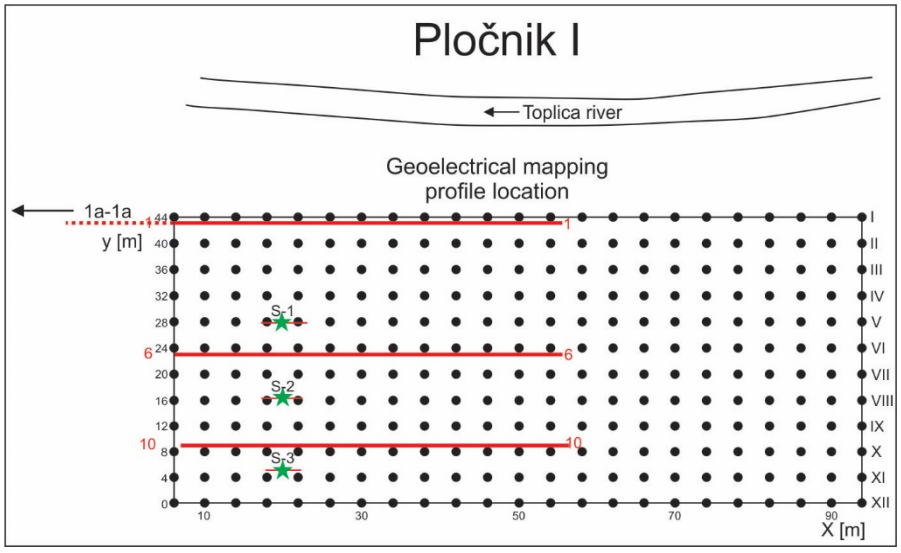

Fig. 2. – Locations of geoelectrical mapping profiles (I-XII), 2D electrical imaging profiles (1-1, 1a-1a, 6-6, 10- 10) and geoelectrical sounding locations (S-1, S-2, S-3).

profiles (1-1, 1a-1a, 6-6, 10-10), and three VES locations used in total (S-1, S-2 and S-3).

The presence of a thin, low resistivity layer that overlays a high resistivity substratum is indicated by 1D interpretation of measured geoelectrical sounding curves with a relatively shallow depth of investigation (AB/2max = 20 m) (Figure 3). The current electrode crossing over local near surface inhomogeneities causes distinct lateral effects in the geoelectrical sounding curve S-1, particularly in the near surface part of the diagram (AB/2= 1.5 m to AB/2 = 3 m). As a result, 1D inversion is not used to interpret the S-1 sounding curve.

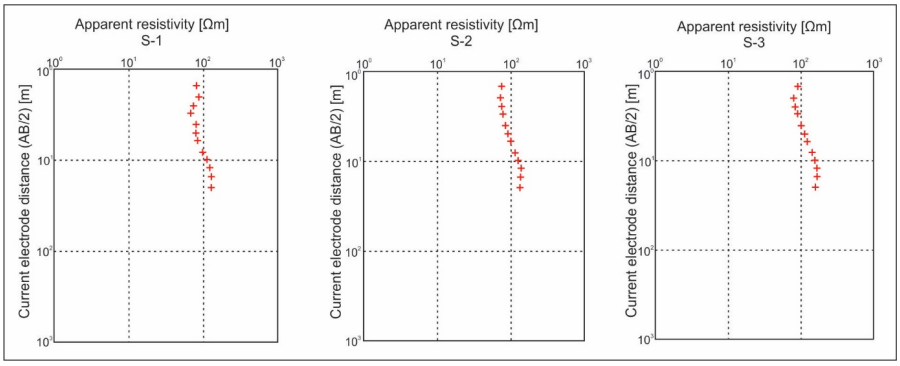

Fig. 3. – Measured sounding curves S-1, S-2 and S-3.

The sounding curve S-3 was interpreted in two different ways, yielding two equivalent models that are shown in Figure 4. In both cases, a low resistivity layer with a thickness of 0.8 meters and a resistivity of about 35 Ωm is present.

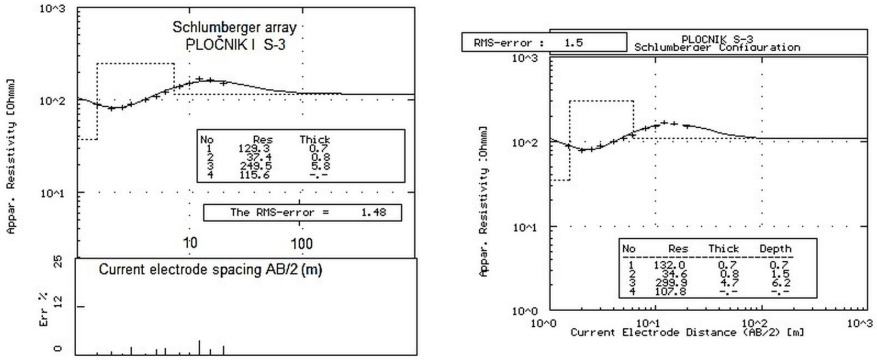

Fig. 4. – Equivalent 1D models obtained after inversion for the sounding curve S-3.

The measurement arrays were oriented parallel to the strike of the vertical cliff formed by Toplica River erosion (with a height of 4 to 5 meters). At sounding station S-3, the cliff's effect is the smallest. The

topography effect would first appear as an increase in measured apparent resistivity values as the Schlumberger array dimensions were increased, followed by a descending trend (Figure 5). In practice, the topographic effect will produce effects similar to the change in resistivity with depth, or a K-type sounding curve. The magnitude of this effect is determined by the cliff height-to-sounding-station-distance ratio (H/X), as well as the cliff angle (the highest being for $\alpha = 90°$). The topographic effect is practically absent as the distance between the sounding station S-3 and the cliff increases (around 40 meters) (Figure 5). Holcombe & Jiracek (1984)

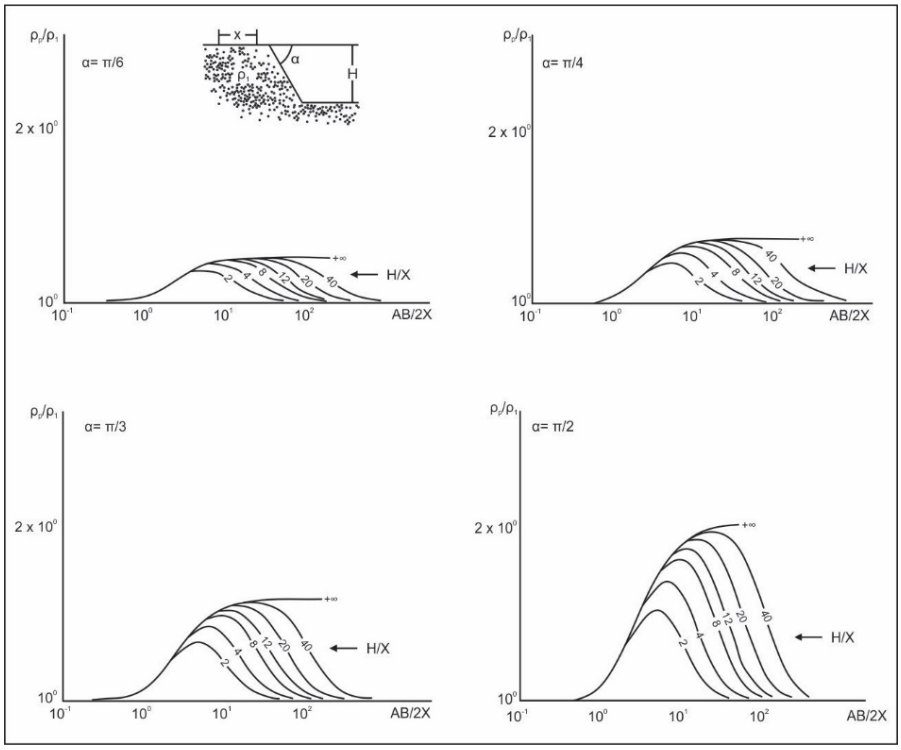

Fig. 5. – Topographic effect of the cliff (array orientation is parallel to the cliff strike).

developed a three-dimensional numerical model that demonstrated the possibility of removing the topographic effect from resistivity data.

2D GEOLECTRICAL SURVEY RESULTS

The apparent resistivity map (Figure 6) showed two distinct resistivity regions, which were apparently separated by a steeply dipping boundary (in the zone of 25-35 meters). The contact between the lower resistivity zone

(yellow zone with resistivity values of 55 to 70 Ωm) and the higher resistivity zone (red zone with apparent resistivity values up to 140 Ωm) is essentially two-dimensional. Three anomalies are indicated within the high resistivity region, indicating the existence of 3D structures. On the apparent resistivity map, the topographic effect of the vertical cliff can be seen as an increase in apparent resistivity values in the vicinity of the cliff (upper part of the map, blue rectangle). The apparent resistivity map was also used to position the 2D electrical imaging profiles (1-1, 1a-1a, 6-6 and 10-10 in Figure 2) for thorough inspection of the most interesting zones (3 closed anomalies) and 2D interpretation of the apparent resistivity pseudosections.

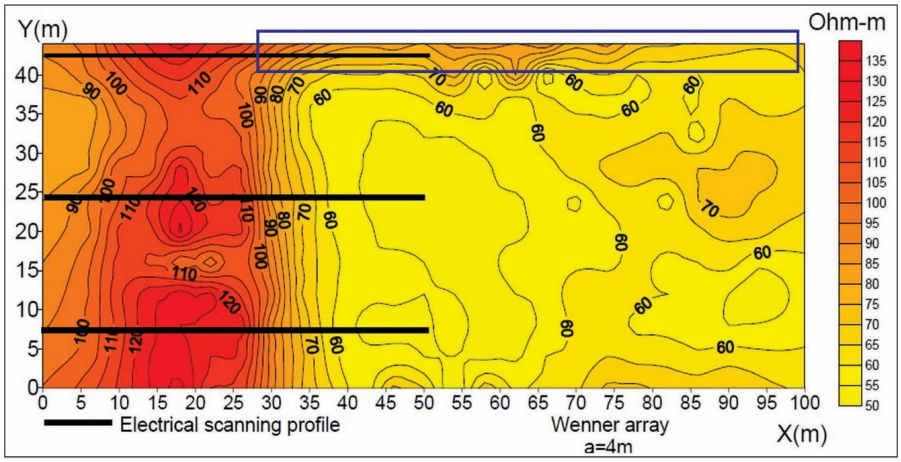

Fig. 6. – Apparent resistivity map constructed with the grid given at Figure 2 (measurements are attached to the midpoint of every Wenner array during the geoelectrical mapping, the length of the Wenner array is a= 4m, with the mapping step ΔX= 4m).

2D electrical imaging method with 26 electrodes (unit electrode spacing a = 2m) was used to further investigate the contact between the two regions, as well as to obtain information about the depth extent and shape of the structures causing 3D anomalies. Surveying was first carried out at five depth levels, along three parallel profiles that were set perpendicular to the 2D contact. Despite the fact that the structures within the high resistivity region are 3D, the results of 2D interpretation were satisfactory (Figure 7). The resistivity of the sources of anomalies is several hundred Ωm, according to two-dimensional models. The highest true resistivity values, as defined by profile 1-1, are influenced in part by the presence of a vertical cliff, as shown on the apparent resistivity map (Figure 6). The same value scale was used for all three profiles during the construction of the 2D

models, which influenced the appearance of the 2D models with lower resistivity ranges (profiles 6-6 and 10-10).

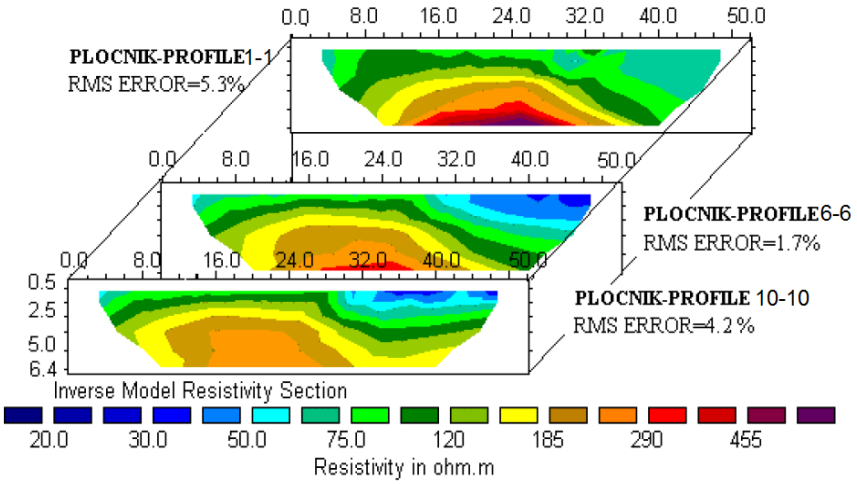

Fig. 7. – Results of 2D inversion along three parallel profiles (1-1, 6-6 and 10-10).

Figure 8 displays the result of 2D inversion along the electrical scanning profile 6-6 with a value scale that better illustrates the subsurface architecture.

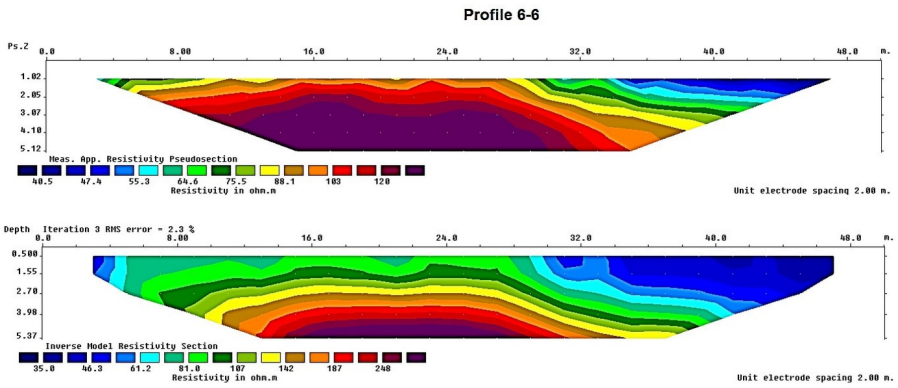

Fig. 8. – Result of 2D inversion along profile 6-6 (bottom) and the measured apparent resistivity pseudosection (top).

Since the results show that the high resistivity zone sinks before the start of the 2D profile, additional measurements, such as the extension of profile 1-1, were taken (Figure 9). In comparison to the subsurface

architecture shown along profile 1-1, the extended results indicate a much simpler subsurface model (close to 1D conditions).

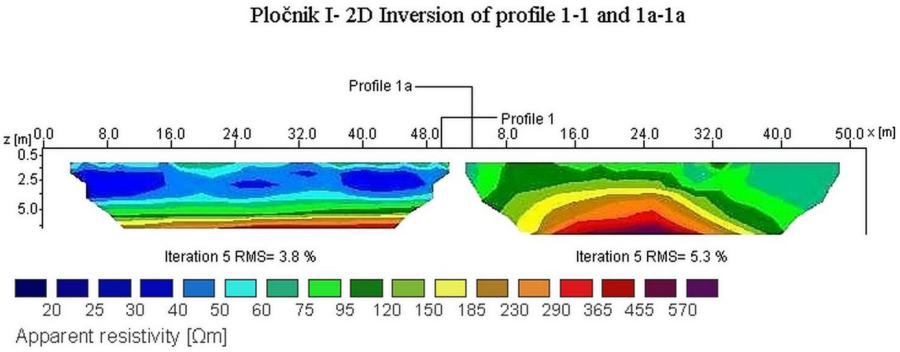

Fig. 9. – Results of inversion along profile 1-1 and its extension 1a-1a.

2D FORWARD MODELLING AND MODEL REFINEMENT

Figure 10 shows two possible models for the entire profile 1-1 and 1a-1a, both of which include the high resistivity pit. An apparent resistivity section was calculated using the forward modeling method (in RES2DMOD, Loke 2016b). This section was later used to invert calculated data and to obtain a 2D model using these calculated data as "measured" apparent resistivity data (in RES2DINV, Loke 2016a).

Based on the analysis that contains forward and inverse modelling it is clear that pits, regardless of their geometry and dimensions cannot be differentiated from the higher resistivity substratum even when they are located at relatively shallower depths and have a high resistivity contrast relative to the surrounding medium. The presence of the pit unambiguously leads to distinct anomalies relative to the simple, 1D geological profile that has been detected along profile line 1a-1a.

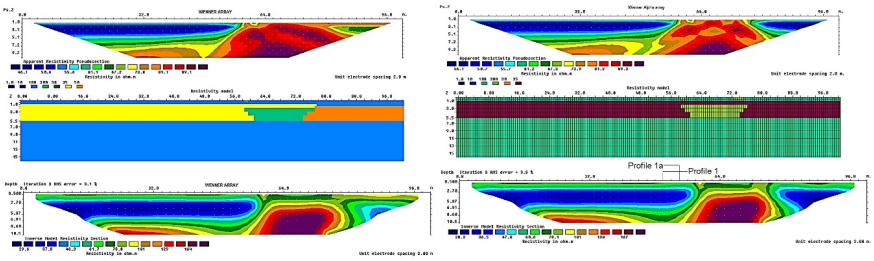

Fig. 10. – Two possible models for the combined profiles 1-1 and 1a-1a (middle), apparent resistivity sections (top) and 2D models obtained after inversion (bottom).

The option "Refine model" was used to perform a 2D inversion along profile 6-6, which allows for a more detailed investigation of near-surface inhomogeneities. The cell width is half the unit electrode spacing when this option is selected. Figure 11 shows the effects of that inversion process when data from all five depth levels are used (Figure 11, top) and when data from just four depth levels are used (Figure 11, bottom). The use of four depth levels is intended to help distinguish the pit from the high resistivity substratum (gravel from the Toplica River).

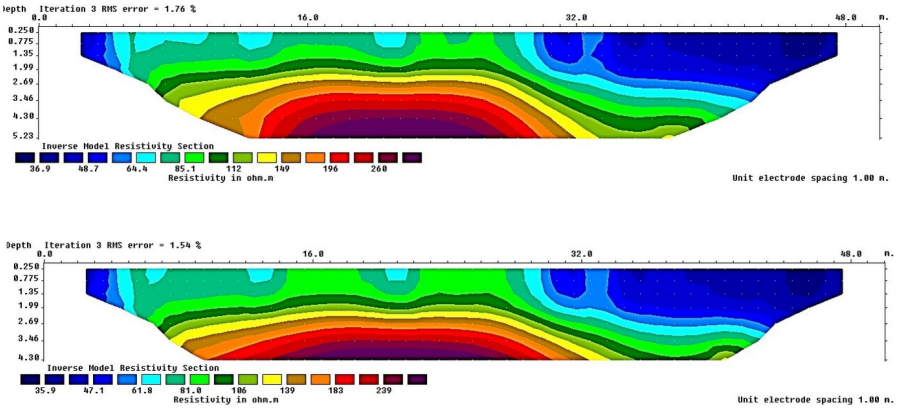

Fig. 11. – 2D inversion of profile 6-6 with the “Refine model” option enabled.

In order to focus on the zone containing the high resistivity anomaly, a 2D inversion of a symmetrically shortened profile 6-6 (first electrode at the 6th meter, last electrode at the 44th meter) was performed. In this case, the “Refine model” option was used, but it did not clearly distinguish the pit from the high resistivity substratum (Figure 12). The usage of the "Refine model" is responsible for the high resistivity surfacing. This option can also be used when looking for other archeological artifacts (other shallower pits etc.).

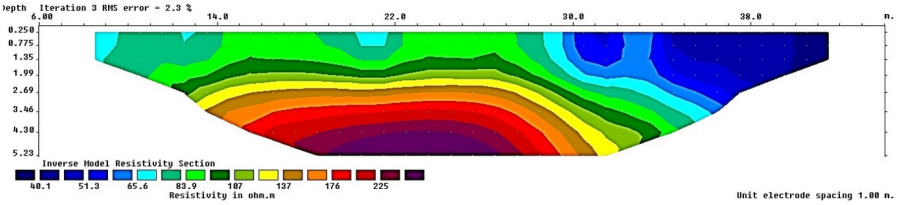

Fig. 12. – 2D inversion along the symmetrically shortened profile 6-6 with the “Refine model” option enabled.

The anomalous zone caused by the presence of the high resistivity pit filled with metallurgy byproducts (ash, slag etc.) was successfully singled out by 2D inversion of an unsymmetrically shortened profile 6-6 (first

electrode at the 0 meter, and the last at the 40th meter) (Figure 13). In this case, the "Refine model" option was also used, which highlighted near-surface inhomogeneities (ripple near surface effect). As a result, the 2D model of true resistivity values is shown in linear scale with two equidistance values (20 and 22.5 Ωm) to reduce the near-surface inhomogeneity effect and highlight the high resistivity anomaly induced by the survey objective (pit).

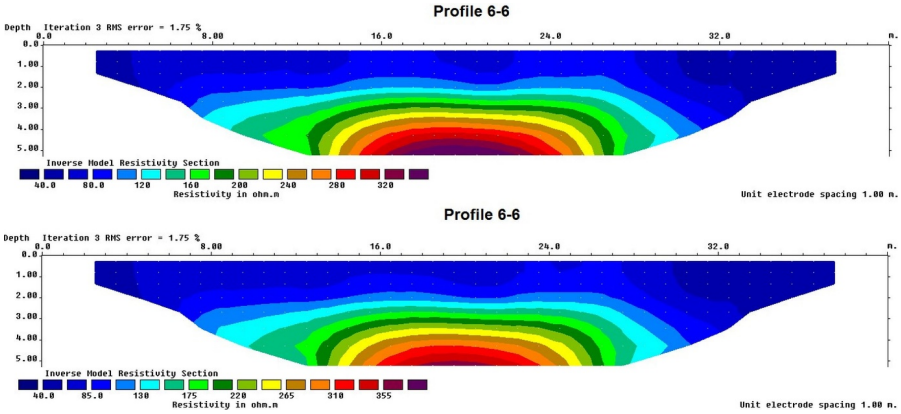

Fig. 13. – 2D inversion of the unsymmetrically shortened profile 6-6 with the "Refine model" option enabled.

Shortening the profile 6-6 (to a total length of 36 meters) resulted in a 2D profile containing only the high resistivity region and not the normal, undisturbed surrounding mediums (loess like clays that lie on top of gravel from the Toplica River). Figure 14a shows the measured apparent resistivity section, which only includes the high resistivity zone from figure 6 (the only exception being the near surface zones at the start and the end of the profile). The measured data clearly do not include data from the deeper lying gravel in the undisturbed zone; instead, they only include data from the anomalous pit zone. The results of 2D inversion were seen in both linear and logarithmic scales (Figure 14b, equidistance of 20 Ωm) (figure 14c, equidistance is increased by 14.5 percent). In both cases, equidistance is chosen to provide a visual representation of the model that does not obliterate any interesting zones. The logarithmic value scale of apparent resistivity best represents information about the near surface region. The high resistivity anomaly (ash pit) has lateral extent of about 10 meters, which corresponds to knowledge about the pit's geometry. The obvious resistivity method's vertical resolution makes it impossible to distinguish between the pit and gravel anomalies. Since the pit is in the lower part of the archeological profile, very close to the alluvium of the Toplica River (Figure 1b), no geophysical method enables the resolution to distinguish the

two anomalies. The other method used was ground penetrating radar (GPR), which was unable to distinguish between the two anomalies.

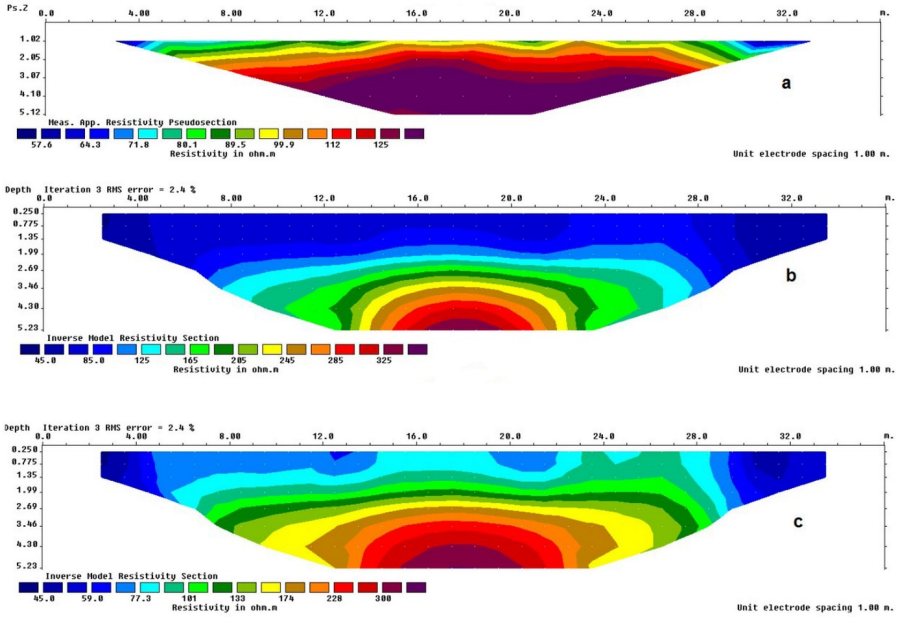

Fig. 14. – (a) Measured apparent resistivity pseudosection; (b) 2D model obtained after inversion with a linear value scale; (c) 2D model obtained after inversion with a logarithmic value scale.

GROUND PENETRATING RADAR SURVEY

Figure 15 shows maps of reflection amplitudes of electromagnetic waves at various two-way travel times (TWT= 15 ns, TWT= 18 ns, and TWT= 22 ns). Only when the TWT value is 18 ns can a contact between high and low resistivity zones be seen on the GPR map of reflection amplitudes as brighter shades. The poor quality of GPR amplitude map results can be interpreted in two ways. First, the presence of a thin low resistivity layer (second layer, thickness 0.8 meters, and resistivity of 35 Ωm) detected with 1D inversion of sounding curve S-3 could cause significant attenuation of the electromagnetic signal. In addition to this, the fact that the subsurface is made up of loess-like clay indicates the presence of fairly homogeneous medium with no permittivity discontinuities, which is a key physical property that determines the magnitude of amplitudes of a GPR section. The GPR method did not yield satisfactory results despite the existence of a relatively high resistivity pit.

3D FORWARD AND INVERSE MODELLING OF THE ANOMALOUS ZONE

The high resistivity zone (depicted as red zone) on Figure 15 (left) could be caused by three distinct anomalous bodies with a 3D geometry but creating a 2D-like contact on the apparent resistivity map. Figure 16 shows

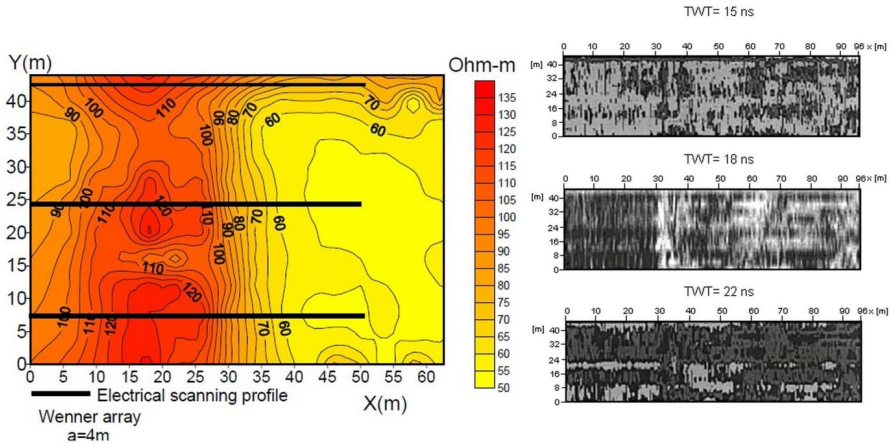

Fig. 15. – Apparent resistivity map (left) and GPR amplitude map obtained for different TWT (right).

a 3D model with a 1.1-meter-thick surface layer and a resistivity of 100 Ωm. The second layer is a low resistivity layer with a thickness of 0.5 meters and a resistivity of 30 Ωm, close to determined resistivity (about 35 Ωm) by the 1D inversion of sounding curve S-3. Three independent, high resistivity (300 Ωm) pits can be seen inside the low resistivity layer. The three pits are conical in shape and reach a depth of 3.2 meters. Finally, a high resistivity substratum (300 Ωm) was modelled at a depth of 4.4 meters, which corresponds to the gravel of the Toplica River alluvium.

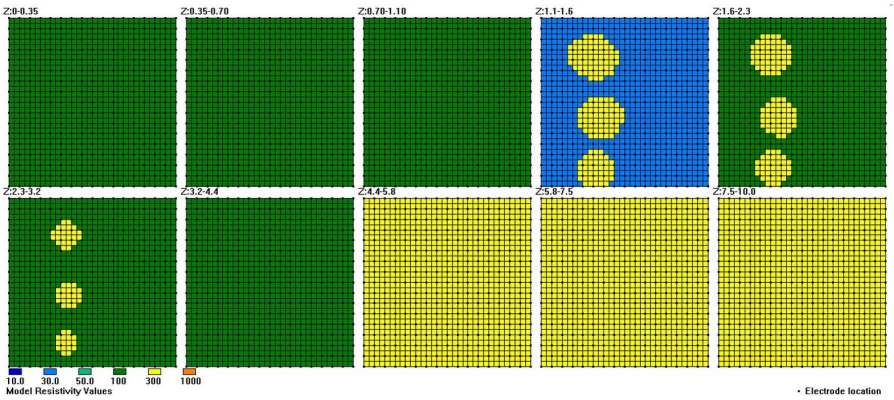

Fig. 16. – 3D forward model of high resistivity pits.

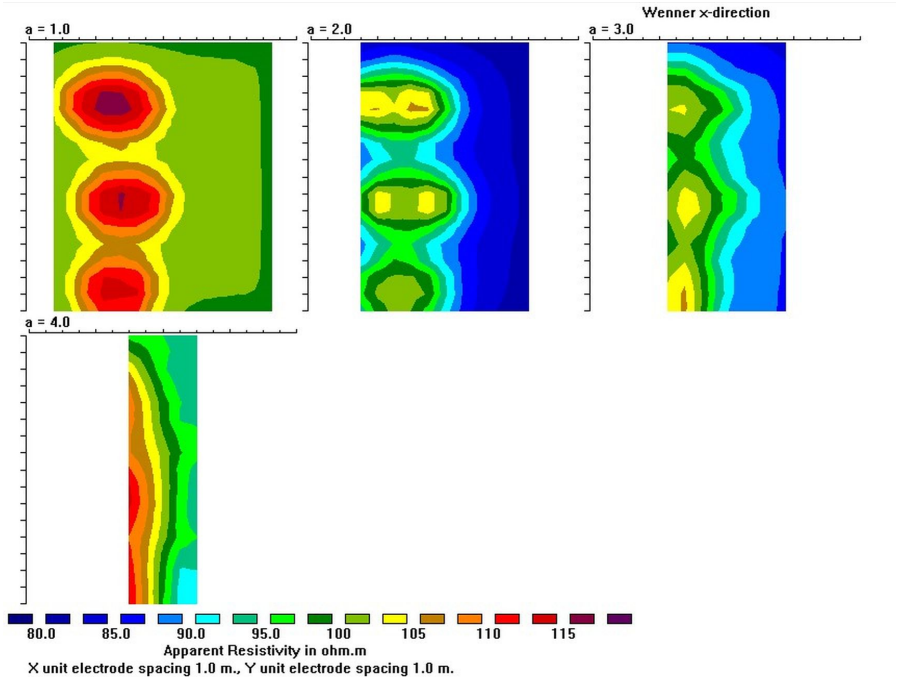

Fig. 17. – Theoretically calculated apparent resistivity maps for the Wenner array.

Figure 17 shows apparent resistivity maps for three array lengths (a = 1m to a = 4m), or three depth levels (from approximately 0.5 meters to 2 meters), when the Wenner array is oriented along the X-axis. As the depth of investigation is increased, the 3D character of the individual anomalies is lost, and the three distinct anomalous zones become one 2D anomalous zone due to a lack of horizontal resolution. When the Wenner array's

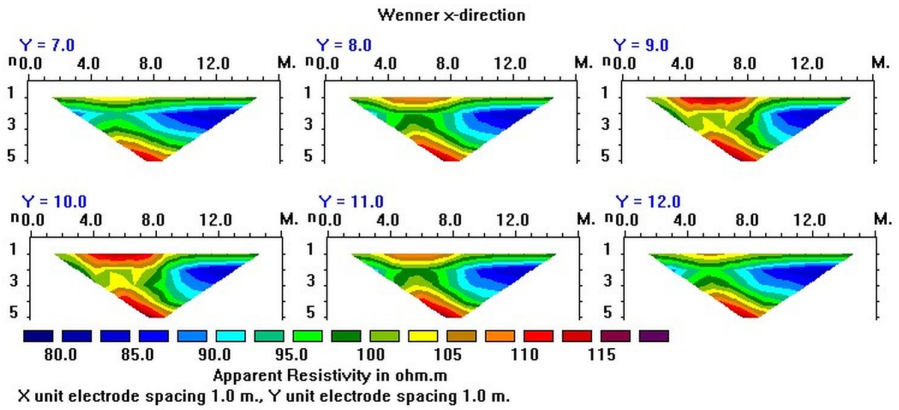

Fig. 18. – Apparent resistivity sections for the Wenner array oriented along the X- axis (Y-axis values range from 7 to 12 meters).

dimensions is a= 4m, the apparent resistivity map from Figure 15 corresponds best with the theoretically calculated apparent resistivity map.

Figure 18 shows apparent resistivity sections that are very similar to 2D survey sections, confirming that the vertical resolution is insufficient to distinguish individual pits from the high resistivity substratum.

The results of a 3D inversion of synthetic data confirm that resolution decreases with depth, and as a result, three individual anomalies are gradually lost as depth increases (Figure 19).

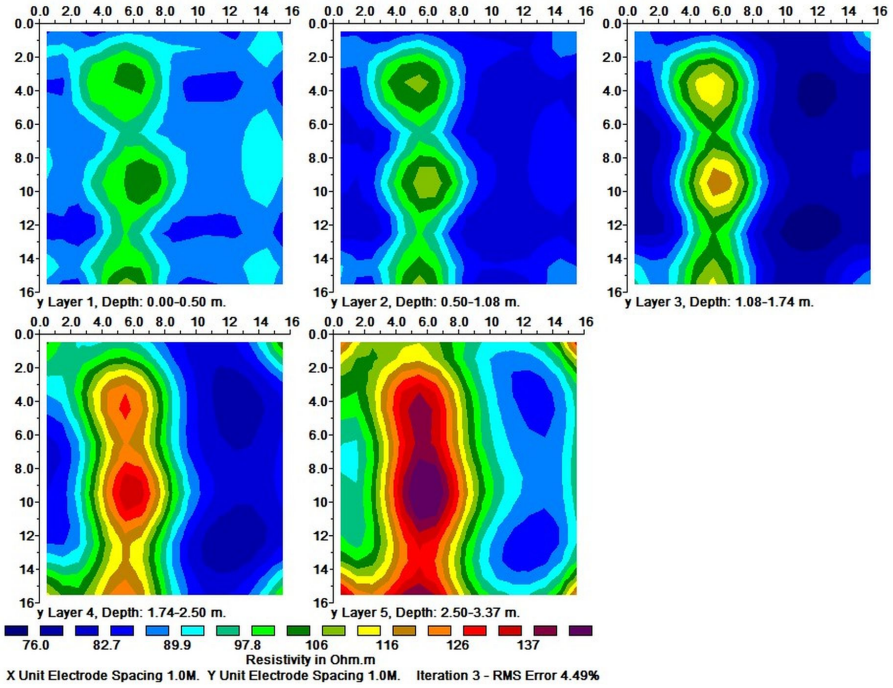

Fig. 19. – 3D model obtained after inversion of synthetic data.

Figures 20 and 21 show maps of 3D inversion using the Pole-pole array for the model shown in figure 16. A Pole-pole array is a two-electrode array in which one potential and one current electrode are separated from the other two electrodes by a large gap (usually ten times the separation of the two measuring electrodes). In comparison to the Wenner array, which is widely used for 2D data acquisition, Pole-pole and Dipole-dipole arrays are commonly used when conducting 3D geoelectrical surveys. The advantages of the Pole-pole array over the Wenner array can be found in better surface coverage which in turn gives a better subsurface image of the 3D anomaly in the high resistivity zone as can be seen from Figures 20 and 21.

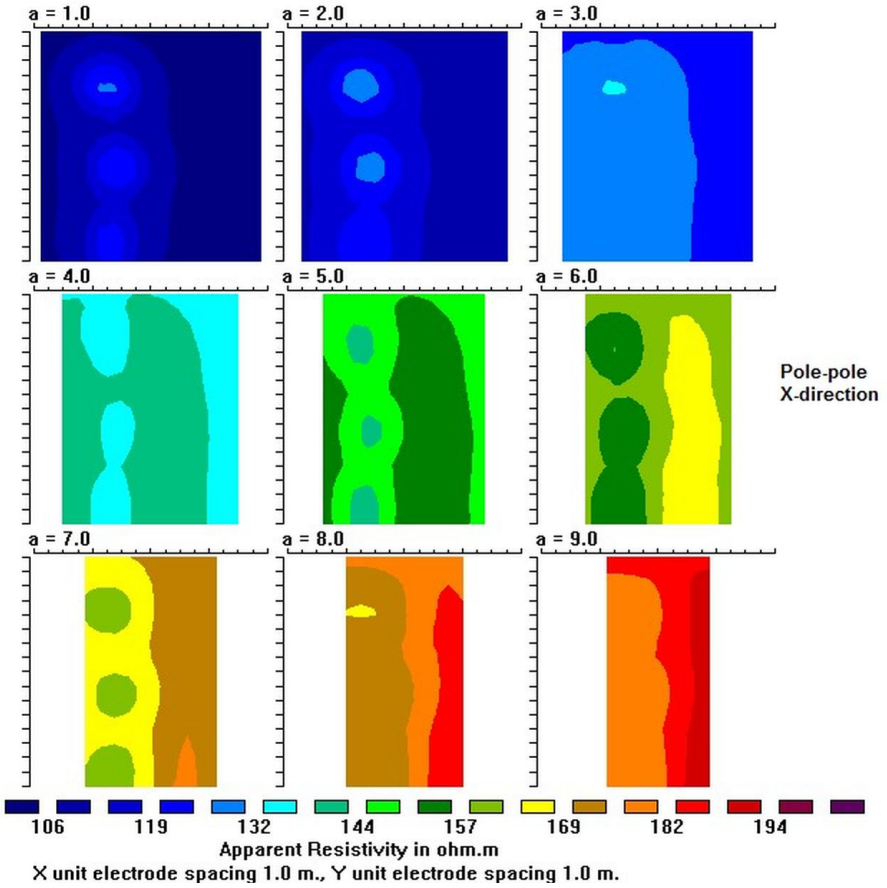

Fig. 20.–Theoretically calculated apparent resistivity maps for the Pole-pole array.

CONCLUSION

The thin, low resistivity layer (0.8 meters, about 35 Ωm) was discovered during 1D geoelectrical survey at sounding station S-3. Low resistivity layer could attenuate electromagnetic wave propagation, which was later determined to be one of the contributors to the low quality GPR results.

The contact between the high resistivity medium and the low resistivity medium was determined using geoelectrical mapping. Following that, 2D electrical imaging profile 1-1 was extended to obtain additional details about the subsurface architecture. The extension of profile 1-1 (1a-1a) was found to have simple, almost 1D subsurface geometry.

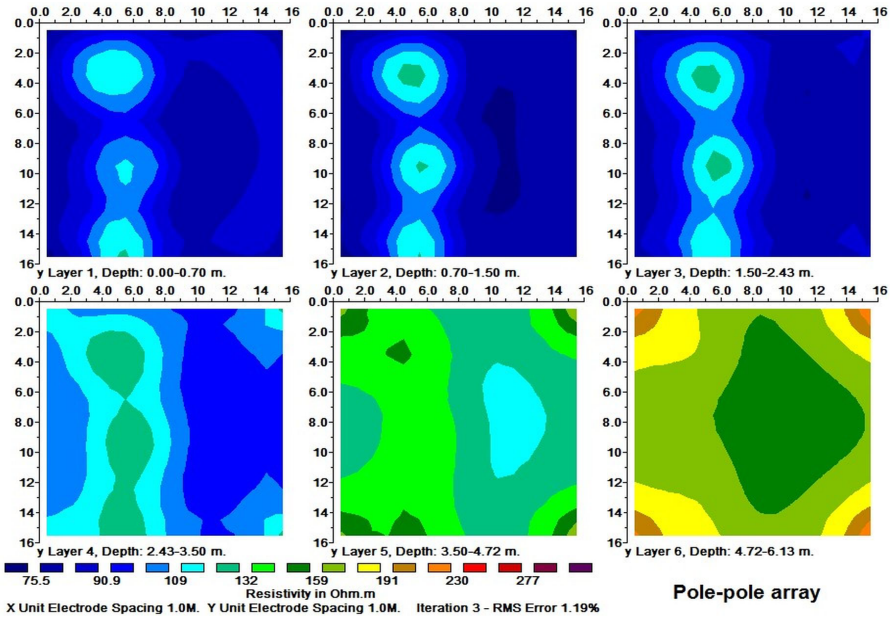

Fig. 21. – 3D model obtained after inversion of synthetic data for the Pole-pole array.

The benefits of model refinement and profile shortening (profile 6-6) were demonstrated with the goal of isolating the high resistivity anomaly. The use of this approach has the disadvantage of illustrating local near-surface inhomogeneities (ripple near-surface effect), which can be less visible by using linear scales and adjusting the equidistance scale. It was also determined that the ERT method's resolution, as well as that of other geophysical methods, is inadequate to distinguish the metallurgy-filled, high-resistance pit from the underlying high-resistance gravel (river Toplica alluvium).

The 3D forward model verified that as depth of investigation increases, three individual anomalies become 2D-like. 3D geoelectrical survey would provide the most accurate subsurface image, but would probably not yield a 3D model where the pits could be distinguished from the underlying high resistivity Toplica River gravel.

REFERENCES

Holcombe, H. T., Jiracek, G. R. (1984): Three-dimensional terrain corrections in resistivity surveys. – Society of Exploration Geophysicist (SEG). – **Geophysics 49 (4)**: 439–452.

Loke, M. H. (2016a): Tutorial: 2D and 3D electrical imaging surveys. – Unpublished revised course notes. http://www.geotomosoft.com/downloads.php

Loke, M. H. (2016b): Rapid 2D resistivity and I.P. forward modeling using the finite-difference and finite-element methods. – Unpublished software manual. http://www.geotomosoft.com/downloads.php

Vukadinovich, S., Sretenovic, B., Sljivar, D. (1999): Combined Geoelectrical and GPR Investigations of the neolithic archealogical settlement "Plocnik" - Serbia. In: 5th EEGS-ES Meeting, September 1999/ 1999 EEGS-ES Abstracts: 35–36. – European Association of Geoscientists & Engineers.

2Д ЕЛЕКТРОМЕТРИЈСКО СКЕНИРАЊЕ НА НЕОЛИТСКОМ НАЛАЗИШТУ "ПЛОЧНИК"

ФИЛИП АРНАУТ, БРАНИСЛАВ СРЕТЕНОВИЋ

Р Е З И М Е

Електрометријска метода скенирања (ERT) коришћена је на локалитету неолитског налазишта „Плочник" у околини Прокупља. Локација сонде вертикалног електричног сондирања (ВЕС) С-3 приказала је нискоотпорну зону дебљине 0,8 метара са вредности специфичне електричне отпорности од око 30 Ωм. Оштра и стрма гранична површ која дели високоотпорну и нискоотпорну средину откривена је методом 2Д геоелектричног картирања. Резолуција електрометријског скенирања проверена је 3Д директним и инверезним моделовањем ради провере могућности диференцирања три индивидуалне високоотпорне јаме од околног високоотпорног шљунка.